Am J Cancer Res 2018;8(4):610-623
www.ajcr.us /ISSN:2156-6976/ajcr0074519

Original Article

A novel 5T4-targeting antibody-drug conjugate H6-DM4 exhibits potent therapeutic efficacy in gastrointestinal tumor xenograft models

Ruixue Wang[1,3*], Qinhuai Lai[1*], Liangze Tang[1], Yiran Tao[1], Yuqin Yao[1,2,3], Yu Liu[1], Ying Lu[1], Chaoyong Shen[4], Ran Lu[5], Chuanwen Fan[6], Ruirui Zhang[1], Yuxi Wang[1], Lin Yu[1], Tinghan Yang[1,4], Yangping Wu[1], Yujia Peng[1], Xian Wei[1,3,7], Yuyin Fu[1], Weirong Lai[1], Lantu Gou[1], Jinliang Yang[1,3]

[1]State Key Laboratory of Biotherapy and Cancer Center/Collaborative Innovation Center for Biotherapy, West China Hospital, Sichuan University, Chengdu, China; [2]Research Center for Public Health and Preventive Medicine, West China School of Public Health and Healthy Food Evaluation Research Center, NO. 4 West China Teaching Hospital, Sichuan University, Chengdu, China; [3]Guangdong Zhongsheng Pharmaceutical Co., Ltd., China; [4]Department of Gastrointestinal Surgery, West China Hospital, Sichuan University, Chengdu, China; [5]Laboratory of Stem Cell Biology, State Key Laboratory of Biotherapy/Collaborative Innovation Center of Biotherapy, West China Hospital, Sichuan University, Chengdu, China; [6]Institute of Digestive Surgery, State Key Laboratory of Biotherapy/Collaborative Innovation Center of Biotherapy, West China Hospital, Sichuan University, Chengdu, China; [7]School of Basic Medical Sciences, Chengdu Medical College, Chengdu, China. [*]Equal contributors.

Received February 13, 2018; Accepted February 25, 2018; Epub April 1, 2018; Published April 15, 2018

Abstract: 5T4, also named as trophoblast glycoprotein, is often upregulated in some cancer cells. Here, we demonstrated that 5T4 was highly expressed in gastric, colorectal, and pancreatic cancer, associated with significantly poor prognosis of gastrointestinal (GI) cancer patients. To search for new targeting drugs for GI cancer, we developed a novel anti-5T4 monoclonal antibody with high affinity and robust internalization ability and conjugated it to the potent microtubule inhibitor DM4 to produce conjugate H6-DM4. This antibody-drug conjugate (ADC) displayed significant cytotoxicity in a panel of GI cancer cell lines with IC_{50} values in the nanomolar range. H6-DM4 eradicated established GI tumor xenograft models at 2.5 mg/kg or 10 mg/kg without observable toxicity. Further, 5T4 was highly expressed in cancer-initiating cells (CICs) compared with non-CICs in colorectal cancer. *In vitro* and *in vivo*, treatment with H6-DM4 exhibited a powerful efficacy on colorectal CICs. Additionally, colorectal cancer cells resistant to platinum were effectively eliminated by H6-DM4. Taken together, our results showed 5T4-positive GI cancer cells, colorectal cancer-initiating cells, and platinum-resistant colorectal cancer cells were potently eliminated by H6-DM4, indicating H6-DM4 may be a potential candidate drug for GI cancer treatment.

Keywords: 5T4, gastrointestinal cancer, antibody-drug conjugate, DM4, targeted therapy

Introduction

Gastrointestinal (GI) cancer, including gastric, colorectal, pancreatic cancer, etc., is the main cause of cancer-related deaths. Gastric cancer has a high incidence in Asia with limited effective drugs available for the middle and late-stage tumors [1, 2]. Colorectal cancer is the third leading cause of cancer mortality worldwide. Thanks to advances in targeting drugs, the five-year survival rate has greatly improved. However, colorectal cancer patients still face a high risk of resistance and recurrence [3, 4]. Pancreatic cancer is a highly malignant tumor with an estimated five-year survival of less than 5%. Moreover, there has been no effective drug up to date. It is rather evident that more effective while less toxic therapies are urgently needed for GI cancer patients [5, 6].

Antibody-drug conjugates (ADCs), combination of high efficiency of chemotherapy drug and specificity of antibody, are innovative drugs for cancer therapy. In recent years, several FDA-approved ADC drugs have obtained encouraging results. For example, ADCETRIS, composed of the anti-CD30 antibody and the microtubu-

le inhibitor monomethyl auristatin E, is an effective treatment for patients with relapsed or refractory Hodgkin's lymphoma. KADCYLA, consisting of trastuzumab and microtubule inhibitor DM1, has been approved for HER2-positive unresectable, locally advanced or metastatic breast cancer [7, 8]. However, there has been no ADC drug for GI cancer in clinic. Therefore, it may be a viable strategy to develop ADC drugs for GI cancer.

5T4 is overexpressed in some cancers such as breast cancer, lung carcinoma, and renal cancer, but has very limited normal tissue expression [9-11]. Moreover, 5T4 elevation correlates with poor prognosis in tumors such as head and neck tumor, colorectal carcinoma, etc [12, 13]. Recent studies have demonstrated that patients with relapse had a higher proportion of 5T4-positive B cell blasts in lymphoblastic leukemia [14]. 5T4 expression in cancer stem cells (CSCs) correlates with poor overall outcomes in NSCLC, which might be responsible for tumor metastasis, resistance, and recurrence [15-17]. Under normal circumstances, 5T4 is primarily expressed in embryonic cells to enhance the chemotaxis and play a key role in embryonic development and cell differentiation [18, 19]. Pathologically, overexpression of 5T4 is associated with E-cadherin down-regulation, resulting in metastatic spread of epithelial tumors [20]. 5T4 is also involved in modulation of β-catenin-independent Wnt signaling by regulating in LRP6 subcellular localization [21]. In addition, 5T4 regulates CXCL12/CXCR4 chemokine mediated chemotaxis, which could promote 5T4-positive tumor cells spreading [22, 23].

An anti-5T4 antibody conjugated to microtubule inhibitor MMAF or DNA inhibitor PBD could induce regression of some solid tumors such as lung cancer and head and neck cancer in mouse models [12, 24], indicating 5T4 is a potential target for cancer therapy. In this study, we identified that high expression of 5T4 in GI cancer patients was significantly associated with shorter overall survival, which prompted us to explore a 5T4-targeting ADC for gastrointestinal cancer. We developed a novel ADC H6-DM4 with high affinity and internalization rate and focused on the antitumor efficacy of H6-DM4 on GI cancer. H6-DM4 efficiently killed 5T4-positive GI cancer cells, colorectal cancer-initiating cells, and cancer cells resistant to chemotherapy *in vitro* and *in vivo*, showing impressive therapeutic efficacy in GI cancer.

Materials and methods

Cell lines

All cell lines (human pancreatic carcinoma cell lines PANC-1, SW1990, BX-PC3, and AsPC-1; human gastric cancer cell lines AGS and HGC-27; human colorectal carcinoma cell lines HT-29, DLD-1, HCT116, LoVo, SW-480, SW-620, and HCT-15; Chinese hamster ovary cell line) were obtained from ATCC. HCT116-Oxaliplatin and SW-480-Oxaliplatin were obtained from West China Hospital. Colorectal CIC3117, CIC3431, and CIC1597 were obtained from Prof. Xianming Mo [25]. All the cell lines were characterized by Feiouer Biotechnology Corporation (Chengdu, China) using short tandem repeat (STR) markers and cultivated at 37°C in a humidified incubator with 5% CO_2 in standard cell culture media as indicated by provider.

Immunohistochemistry (IHC)

Following formalin fixing, paraffin-embedded tissue sections were deparaffinized in xylene and rehydrated in gradient concentration of ethanol. The slides were pretreated with 0.3% hydrogen peroxide in methyl alcohol for 20 min, treated with Target Retrieval Solution for 20 min at 99°C, and incubated with mouse anti-5T4 (R&D, USA) after blocking with goat serum at 4°C overnight. Following a wash, the slides were incubated with horseradish peroxidase-conjugated anti-mouse and rabbit antibody (Dako REAL™ EnVision™ Detection System, USA) for 60 min at room temperature and then visualized using diaminobenzidine tetrahydrochloride.

Flow cytometry (FCM)

FCM (FACSCalibur, BD, USA) was used to determine 5T4 expression in cancer cell lines and patient-derived cancer tissues. NovoExpress software was utilized to process the obtained data. Cultured cells or tissues were digested to single-cell suspensions by trypsin/collagenase and incubated with anti-5T4 antibody H6 (prepared by our group) or isotype IgG (Merk, Germany) for 30 min on ice. After a wash, they

were infiltrated with FITC conjugated goat anti-human second antibody (ZSGB-BIO, China) for 30 min. To identify 5T4 expression in $CD44^{high}CD54^{high}$ and $CD44^{low}CD54^{low}$ populations of colorectal cancer cells separately, CIC3117 and CIC3431 were stained with FITC conjugated mouse anti-CD44 antibody (BD Pharmingen™, USA) and PerCP-eFluor 710 conjugated mouse anti-CD54 antibody (Invitrogen, USA) or corresponding isotype IgG (BD Pharmingen™, USA; Invitrogen, USA). Cells mixed with an anti-5T4 antibody H6 (prepared by our group) or isotype IgG (Merk, Germany) were incubated on ice for 30 minutes, followed by APC conjugated mouse anti-human antibody (BD Pharmingen™, USA) for 30 minutes at 4°C. All samples were washed three times before detection by FCM.

Establishment of 5T4-positive cell lines and expression of recombinant 5T4 protein

The Chinese hamster ovary (CHO) cells were infected with lentivirus containing the full-length human 5T4 encoding cDNA sequence (GeneChem, China) and selected with puromycin (1-10 μg/ml) to produce CHO-$5T4^+$ cell lines. Recombinant human 5T4 extracellular domains (ECD) were produced by HEK293F cells via transient transfection with mammalian expression vectors pTT5 containing 5T4 ECD fused to human IgG-Fc (5T4-ECD-hFc, Genscript, China) or C-terminal His (5T4-ECD-His, Genscript, China). Recombinant proteins were purified by protein A affinity chromatography or nickel column (GE Healthcare, USA).

Generation of anti-5T4 monoclonal antibody

Balb/c mice were immunized with 5T4-ECD-hFc in combination with adjuvants. Hybridoma technology was utilized to obtain anti-5T4 monoclonal antibodies. Binding abilities were first determined by ELISA using 5T4-ECD-His, and then by FCM using CHO-$5T4^+$ cells. Antibodies with high affinity and robust internalization were selected by SPR and FCM.

Internalization assay in vitro

$5T4^+$ cells incubated at 4°C were shown distinct cell surface localization of antibody, and surface membrane localization of antibody was dramatically reduced at 37°C after 4 hours. The degree of internalization of cell surface-bound antibody was determined by the percentage of decrease in mean fluorescence intensity (MFI) of samples incubated at 37°C compared to control samples incubated at 4°C. FCM was used to quantify the internalization of antibodies. The following formula was used to calculate the internalization efficiency of each antibody in cells: internalization efficiency (%) = [(fluorescence intensity of the control group - fluorescence intensity of the experimental group)/fluorescence intensity of the control group] × 100% [26].

SPR method

5T4-ECD-hFc was immobilized onto the surface of CM5 chips by EDC/NHS coupling method. For kinetic analysis, anti-5T4 mAbs with different concentrations were injected into Biacore × 100 (GE Healthcare, USA), diluted with HBS-EP running buffer, whereas another channel was set as control. The experiment was conducted at 25°C; the flow rate was 10 μl/min. The analytes bound on the sensor chips were dissociated by HBS-EP running buffer for 1200 s. Regeneration of the sensor chips was performed for 30 s by 10 mM glycine-HCl buffer (pH = 1.5).

Preparation and characterization of H6-DM4, IgG-DM4, H6-Cy5.5 and IgG-Cy5.5

Through several screening methods including ELISA, SPR and FCM, the hybridoma clone H6 stood out. The variable region of H6 was sequenced and a chimeric antibody was engineered. The potent cytotoxic maytansine derivative DM4 was conjugated to H6 or control IgG (Bioss, China) via a disulfide-bearing linker SPDB to generate conjugate H6-DM4 or IgG-DM4. Briefly, the coupling reactions were performed by adding a 7~10-fold molar excess of the SPDB-DM4 (Accela ChemBio, China) to antibody at a final concentration of 5 mg/mL in PBS with EDTA including 10% DMF (v/v) at room temperature overnight. Amino-based bioconjugation method was conducted to prepare H6-Cy5.5 and IgG-Cy5.5 as the method described above.

In vivo distribution of H6

A DLD-1 xenograft model was established as described in the following section. When the volume of subcutaneous xenografts reached

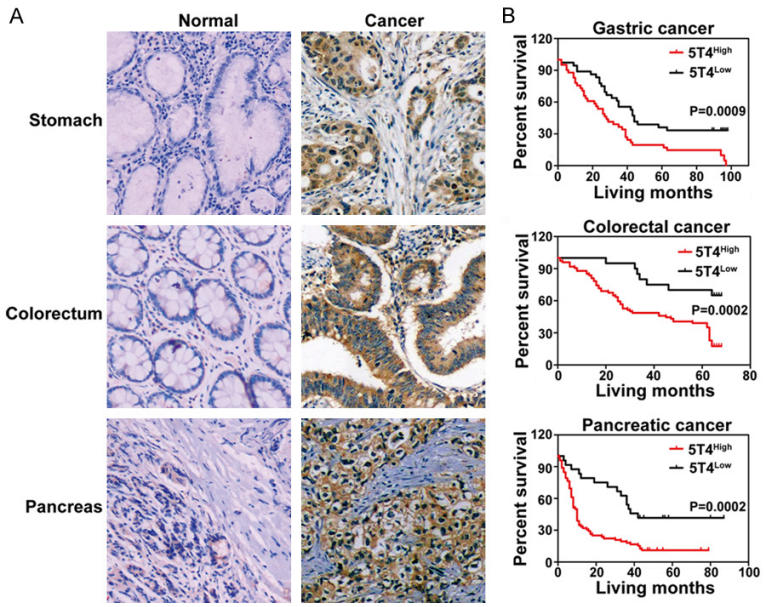

Figure 1. 5T4 protein expression in GI cancer and correlated with poor overall outcomes. A. 5T4 Immunohistochemistry staining in adjacent noncancerous tissues (n = 264 left) and in paired GI cancer tissues (right): gastric cancer (n = 88), colorectal cancer (n = 84), and pancreatic cancer (n = 94). Clinical samples of GI cancer patients were stained for 5T4 antigen (brown stain in membrane or cytoplasm) and counterstained with hematoxylin (blue). Magnification: × 200. B. Patients with $5T4^{high}$ tumors (red line) and $5T4^{low}$ tumors (black line) in correlation with survival time in GI cancer patients.

500 mm^3, these mice were divided into two groups (n = 5). H6 or control IgG (Bioss, China) labeled with Cy5.5 were administered via tail vein injection to mice. At 2, 4, 8, 24, 48 and 72 hour after injection, the distribution of H6 or IgG control *in vivo* was observed by luminescence imaging system.

Orosphere assay

Colorectal CICs had been sorted for $CD44^{high}$ $CD54^{high}$ and $CD44^{low}CD54^{low}$ populations by fluorescence activated cell sorting. Sorted cells were cultured in serum-free DMEM/F12 supplemented with bFGF and rhEGF (Peprotech, USA). Cells were seeded at 1000 cells per well in 96 well ultra-low attachment plates (Corning, USA). Spheres of 50 cells or more were counted after seven days.

In vitro cytotoxicity

To determine *in vitro* cytotoxicity, tumor cells or colorectal CICs were incubated with various concentrations of drugs. Cell viability was measured at 72 hour using Cell Counting Kit-8 (Dojindo, Japan). GraphPad Prism® was used to calculate the half maximal inhibitory concentration (IC_{50}) of drugs on tumor cells.

In vivo treatment

Four to six-week-old female immune-deficient mice (Hfk-bio, China) were maintained according to the Institutional Animal Care and Treatment Committee of State Key Laboratory of Biotherapy in Sichuan University. Balb/c nude mice were implanted with HT-29, HGC-27, HCT-15, DLD-1, SW-480-Oxaliplatin, and colorectal CIC3117. NOD-SCID mice were implanted with PANC-1 and BX-PC3 cancer cells. For the pancreatic PDX-954 model, NSG mice were implanted with three to five mm^3 passage 4 (P4) pancreatictumorfragments(Biocytogen, China). They were randomized into groups of five to eight mice when tumors reached a size of approximately 300 mm^3. Mice were treated with either H6-DM4 (10 mg/kg or 2.5 mg/kg), control (10 mg/kg of H6 or IgG-DM4), vehicle (PBS) or oxaliplatin (10 mg/kg) intravenously with 3 doses given at 3-day intervals. Tumor volumes were recorded twice weekly according to the formula $(width)^2$*height/2. Mice were sacrificed when tumors reached a mean volume of 2000 mm^3.

Statistical analyses

Statistical analyses were performed using GraphPad Prism version 5 (GraphPad Software Inc, USA). Overall survival data were analyzed and plotted using the Kaplan-Meier method. Survival curves were compared using the log-rank test. Individual or multiple group comparisons were performed by 2-tailed Student's t-test or ANOVA-Tukey. The associations between 5T4 expression and pathological grading/clinical staging were analyzed using Chi-squared test. Correlation was tested by Spearman's Rank Correlation Test. Bars exhibited on vertical scatter plots represent the geometric mean or mean for each group. Differ-

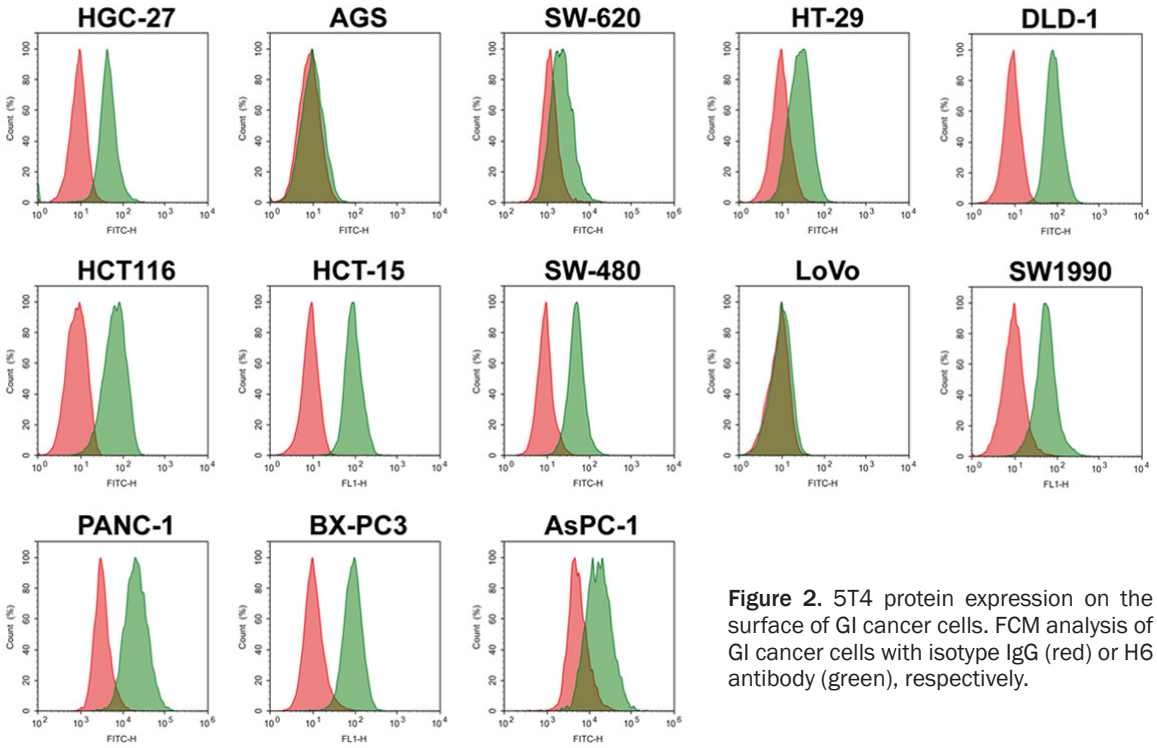

Figure 2. 5T4 protein expression on the surface of GI cancer cells. FCM analysis of GI cancer cells with isotype IgG (red) or H6 antibody (green), respectively.

ences in all comparisons were considered statistically significant at P values < 0.05.

Results

5T4 expression correlated with survival of GI cancer patients

To make sure the suitability of 5T4 for antibody-directed drug targeting for GI cancer, expression of 5T4 was analyzed by IHC staining of human GI cancer tissue and normal tissue microarrays. Gastric cancer tissues, colorectal cancer tissues, and pancreatic cancer tissues demonstrated elevated 5T4 expression levels compared to normal tissues exhibited (P < 0.001). 5T4 staining was positive at any staining in 89.8% (79/88) of gastric cancer samples, 91.7% (77/84) of colorectal cancer samples, and 98.9% (93/94) of pancreatic cancer samples. In contrast, there was a limited expression in normal GI tissues except the glands (**Figure 1A**). In pancreatic cancer, 5T4 is primarily expressed on plasma membrane with limited staining on cytoplasm but is equally distributed on both cell membranes and cytoplasm in gastric and colorectal cancer. The 5T4 expression levels correlated with pathological grading in pancreatic cancer (P < 0.01) and clinical staging in colorectal cancer (P < 0.05, Supplementary Figure 1). Furthermore, the survival analysis showed that higher 5T4 expression in GI cancer patients was associated with significantly lower survival (P < 0.001, **Figure 1B**).

5T4 expression on the cell surface of GI cancer cells

In an effort to identify 5T4 expression on the cell surface of GI cancer, thirteen cell lines were employed to determine 5T4 expression by FCM. High expression of 5T4 was detected in seven cell lines by FCM. Four cell lines showed a low level of expression, while the remaining two cell lines had no expression (**Figure 2** and **Table 1**). The relative expression levels of each cell line were demonstrated in **Figure 2** and **Table 1**. Based on these results, we chose cell lines with high, middle, and low expression of 5T4 to evaluate the antitumor activity of H6-DM4 *in vitro* and *in vivo*.

Generation and characterization of H6-DM4

Recombinant 5T4-ECD-hFc was employed to immune mice and to produce mouse monoclonal antibodies. The binding, affinity, and inter-

Table 1. *In vitro* potency of H6-DM4 in GI cancer cell lines with different expression levels of 5T4

Cell lines	Cancer types	Relative expression of 5T4	*In vitro* potency (IC_{50}) of H6-DM4 (nM)
PANC-1	Pancreatic cancer	11.9	37.58
HCT-15	Colorectal cancer	10.3	74.76
DLD-1	Colorectal cancer	9.6	0.53
HCT116	Colorectal cancer	8.56	19.37
BX-PC3	Pancreatic cancer	7.8	1.74
SW1990	Pancreatic cancer	6.1	28.26
SW-480	Colorectal cancer	5.5	16.84
HGC-27	Gastric cancer	5.1	14.16
AsPC-1	Pancreatic cancer	3.4	23.26
HT-29	Colorectal cancer	2.9	3.89
SW-620	Colorectal cancer	2.0	16.39
LoVo	Colorectal cancer	1.0[a]	> 300
AGS	Gastric cancer	1.0[a]	n.d.[b]

[a]For purposes of comparison, the expression level of 5T4-negative cells such as LoVo and AGS was assigned the value of "1", calculated by the formula: mean fluorescence intensity of H6 antibody group/mean fluorescence intensity of control IgG group, and other cells were expressed relative to that value. The following formula was used to calculate the relative expression of 5T4 in GI cancer cell lines: relative expression level = (mean fluorescence intensity of H6 antibody group/mean fluorescence intensity of control IgG group)/1. [b]n.d. represent no detection.

nalization ability of some candidate antibodies were shown in Supplementary Figure 2; Supplementary Table 1; Supplementary Figures 3 and 4, respectively. Of these candidates, mAb H6 stood out with high affinity and remarkable internalization ability and therefore was engineered to a chimeric antibody. The affinity of H6 was measured to be $1.871*10^{-11}$ mol/L as confirmed via Biacore analysis (**Figure 3A**). To clarify the tumor-binding activity and distribution of H6-DM4 *in vivo*, Cy5.5 labeled H6 and IgG were administered respectively to tumor-bearing Balb/c nude mice. As expected, H6-Cy5.5 could target tumor tissues rapidly within 2 hours post-injection and fluorescence intensity remained on tumor areas even after 72 hours (**Figure 3B**). Then, H6 antibody was conjugated to the microtubule inhibitor DM4 via sulfhydryl substance-sensitive linker SPDB (**Figure 3C**), resulting in H6-DM4 with an average drug to antibody ratio (DAR) of about 2.7 mol/mol by LC-MS (**Figure 3D**). Binding specificity to CHO-5T4$^+$ cell but not CHO-neo was observed by FCM (**Figure 3E**). And results from FCM showed that the internalization rate was similar between H6 and H6-DM4 in HGC-27 (68% and 65%, respectively) or in DLD-1 cells (46% and 48%) (**Figure 3E**).

H6-DM4 in vitro cytotoxicity

The cytotoxicity of H6-DM4 against a several of human GI cancer cell lines with different levels of 5T4 expression was evaluated in cell killing assays. High potency in nanomolar range was observed in 5T4-positive cancer cells, with IC_{50} values of 0.53 nM against DLD-1, 3.89 nM against HT-29, and 1.74 nM against BXPC3, etc., but poor killing against 5T4-negative LoVo cells with the IC_{50} value of more than 300 nM (**Table 1**). The cytotoxicity of H6-DM4 resulted from delivery of the payload to the tumor cells rather than from the antibody because unconjugated H6 antibody did not inhibit proliferation of tumor cell lines (**Figures 4**, **6E**). In general, the antiproliferative activity of H6-DM4 was dependent on 5T4 expression, but there was no linear correlation observed between 5T4 relative expression levels and ADC potency *in vitro* (**Table 1**).

In vivo antitumor activity of H6-DM4 in 5T4$^+$ GI cancer

GI cancer cells or patient-derived xenografts were implanted subcutaneously in nude mice, NOD-SCID mice or NSG mice in order to test the antitumor activity of H6-DM4. H6-DM4 eradicated seven different GI cancer xenograft models at 2.5 mg/kg or 10 mg/kg (**Figure 5A**, **5B**). H6-DM4 at a dose of 2.5 mg/kg eradicated nearly all mice bearing GI cancer xenografts that expressed high levels of 5T4, such as PANC-1, BX-PC3, HCT-15 and DLD-1. In addition, H6-DM4 induced durable tumor regression lasting ~100 days after the completion of dosing with no tumor recurrence (**Figure 5A**). H6-DM4 at a dose of 10 mg/kg induced complete tumor regression when tumor cells expressed low levels or medium levels of 5T4, such as HGC-27, HT-29 and PDX-954 (**Figure 5A**, **5B**). In contrast to the antitumor activity observed with H6-DM4, little activity was observed with the unconjugated antibody or the

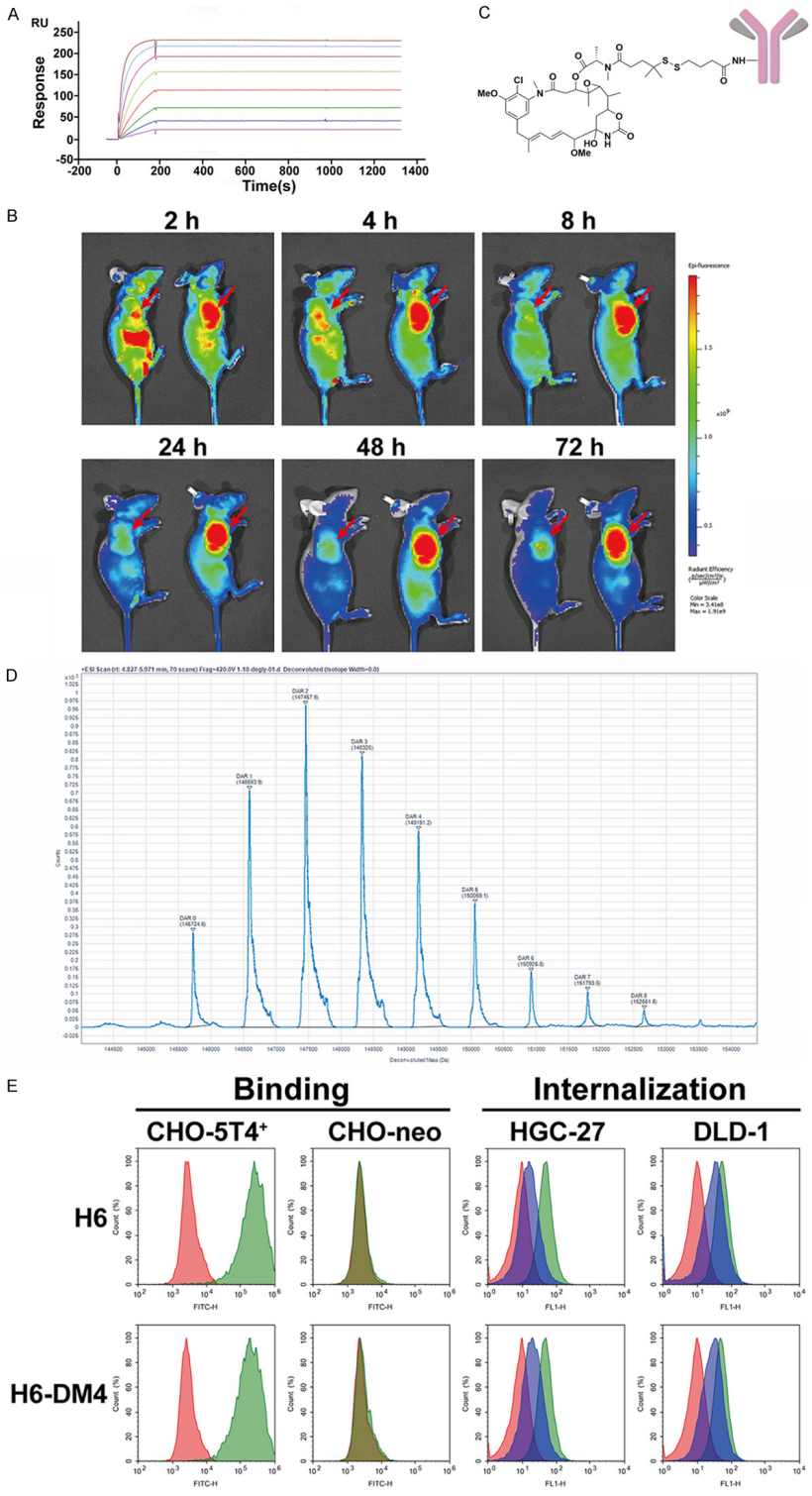

Figure 3. Characterization of H6 antibody and ADC H6-DM4. A. Affinity analysis of the antibody H6 using Biacore (K_D = 1.871*10^{-11}). B. *In vivo* near-infrared imaging of DLD-1 tumor-bearing mice at 2, 4, 8, 24, 48 and 72 hours after injection of hIgG-Cy5.5 (left) and H6-Cy5.5 (right), respectively. Tumors are indicated by red arrows. C. Structure of SPDB-DM4 attached to antibody H6 lysine. D. DAR of H6-DM4 was determined by LC-MS (DAR = 2.7). E. FCM analysis was performed to assess the binding ability of H6 and H6-DM4. CHO-5T4$^+$ and CHO-neo cells with isotype IgG (red) or H6/H6-DM4 (green), respectively; FCM was utilized to evaluate internalization rate of H6 and H6-DM4 in HGC-27 (68% and 65%, respectively) or DLD-1 (46% and 48%, respectively) cells. The red represents cells incubated with isotype IgG; the green with H6 remained on ice; the blue with H6 shifted to 37 °C for 4 h.

control ADC (**Figure 5A**, **5B**). These tumor models represented a broad range of 5T4 expression levels, as determined by FCM and IHC (**Figures 2**, **5B**; **Table 1**; Supplementary Figure 5). A positive correlation was found between the expression levels of 5T4 (intensity detected by FCM) and the *in vivo* efficacy (**Figure 5C**).

H6-DM4 efficacy against colorectal CICs

After proving a powerful therapeutic efficacy of H6-DM4 treatment for 5T4-positive GI cancer, we further investigated whether H6-DM4 performed well in colorectal CICs. First, we detected 5T4 expression in several colorectal CICs separated from colorectal patients by FCM (**Figure 6A**). CD44^{high}CD54^{high} colorectal cancer cells, also known as CICs or CSCs, had higher 5T4 expression compared to non-CICs showed (**Figure 6B**). Dose-dependent decrease of the number of orospheres per well was observed significantly in CIC3117 and CIC3431 seven days after treatment with H6-DM4 com-

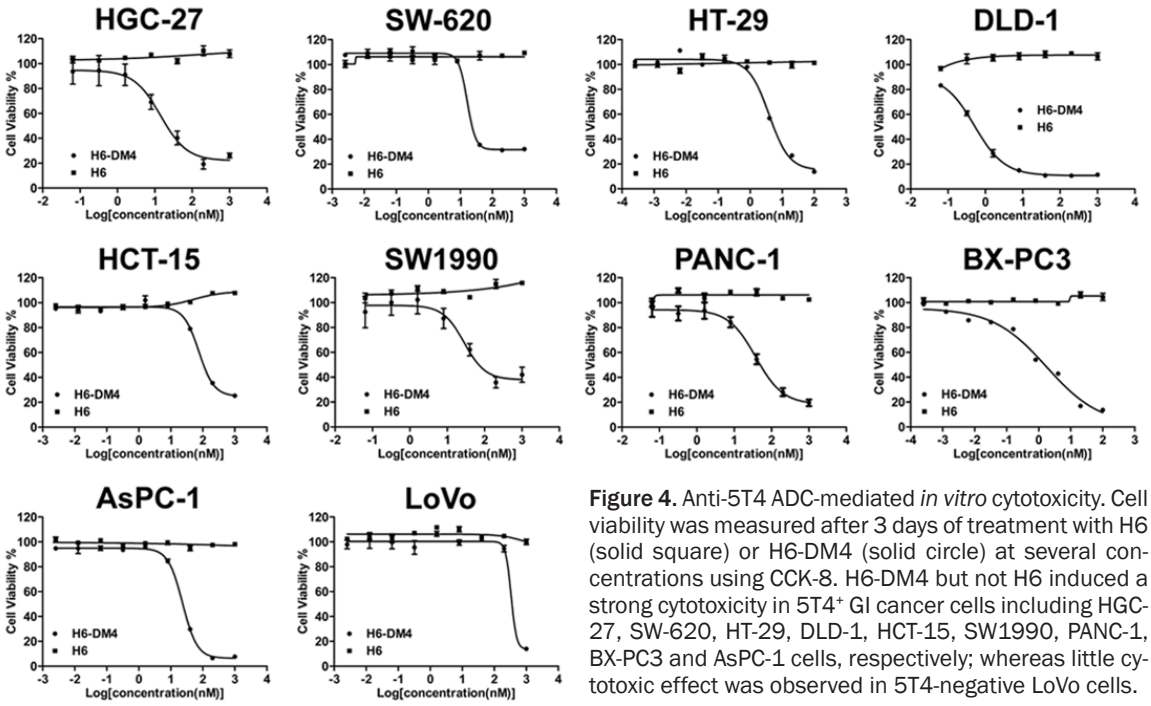

Figure 4. Anti-5T4 ADC-mediated *in vitro* cytotoxicity. Cell viability was measured after 3 days of treatment with H6 (solid square) or H6-DM4 (solid circle) at several concentrations using CCK-8. H6-DM4 but not H6 induced a strong cytotoxicity in 5T4$^+$ GI cancer cells including HGC-27, SW-620, HT-29, DLD-1, HCT-15, SW1990, PANC-1, BX-PC3 and AsPC-1 cells, respectively; whereas little cytotoxic effect was observed in 5T4-negative LoVo cells.

pared to that with H6 at a concentration of as low as 0.064 nM ($P < 0.05$ for each comparison, **Figure 6C**, **6D**). Furthermore, H6-DM4 induced a strong inhibitory activity on colorectal CICs with the IC_{50} values of 0.51 nM against CIC3117, 1.15 nM against CIC3431, and 1.83 nM against CIC1597, respectively (**Figure 6E**). Moreover, H6-DM4 at a dose of 10 mg/kg also showed greater efficacy against CICs-induced xenograft model compared to dose-matched controls ($P < 0.05$). H6-DM4 at a dose of 10 mg/kg eradicated tumor in vivo, while the oxaliplatin or IgG-DM4 group showed slight efficacy (**Figure 6F**). This analysis showed a stronger inhibition of colorectal CICs in the H6-DM4 group ($P < 0.05$) as compared to that in the chemotherapy group.

H6-DM4 potency in platinum-resistant colorectal cancers

Considering the resistance and recurrence of GI cancer, we wanted to challenge H6-DM4 with chemotherapy-resistant colorectal cancer cells. Then, 5T4 expression was examined in colorectal cancer cells resistant to oxaliplatin named SW-480-Oxaliplatin and HCT116-Oxaliplatin (**Figure 7A**). Drug-resistant cells showed ten times more resistant to oxaliplatin than parental cells exhibited (**Figure 7B**). Notably, SW-480-Oxaliplatin and HCT116-Oxaliplatin cells demonstrated the similar sensitivity to H6-DM4 with IC_{50} values of 16.64 nM and 19.4 nM compared with their parental cells indicated (**Figure 7C**). SW-480-Oxaliplatin tumor xenograft was completely repressed by H6-DM4 at 10 mg/kg, while the control ADC, unconjugated mAb or oxaliplatin exhibited little antitumor activity (**Figure 7D**). These data provided evidence that the activity of this ADC depended on targeted delivery of the payload to 5T4-expressing tumor cells.

Preliminary safety of H6-DM4

During the entire treatment period, no significant body weight loss or morbidity were observed (**Figure 8A**). In order to further understand the safety of H6-DM4, the preclinical safety profile of H6-DM4 was characterized in two doses of H6-DM4 (2.5 mg/kg or 10 mg/kg) or PBS (n = 5, Q3D × 3 regiment). The mice were euthanized on day 3 and 29 to evaluate acute and delayed toxicities, respectively. There were no observable marrow suppression or damage to vital organs, with no effects on blood function, liver function or renal function on day 3 (**Figure 8B**, **8C**) and 29 (Supplementary Figure 6), respectively.

Discussion

5T4, specifically overexpressed on the cell surface of a variety of tumors and internalized rapidly when bound to antibody, may be used as an attractive target to develop an effective

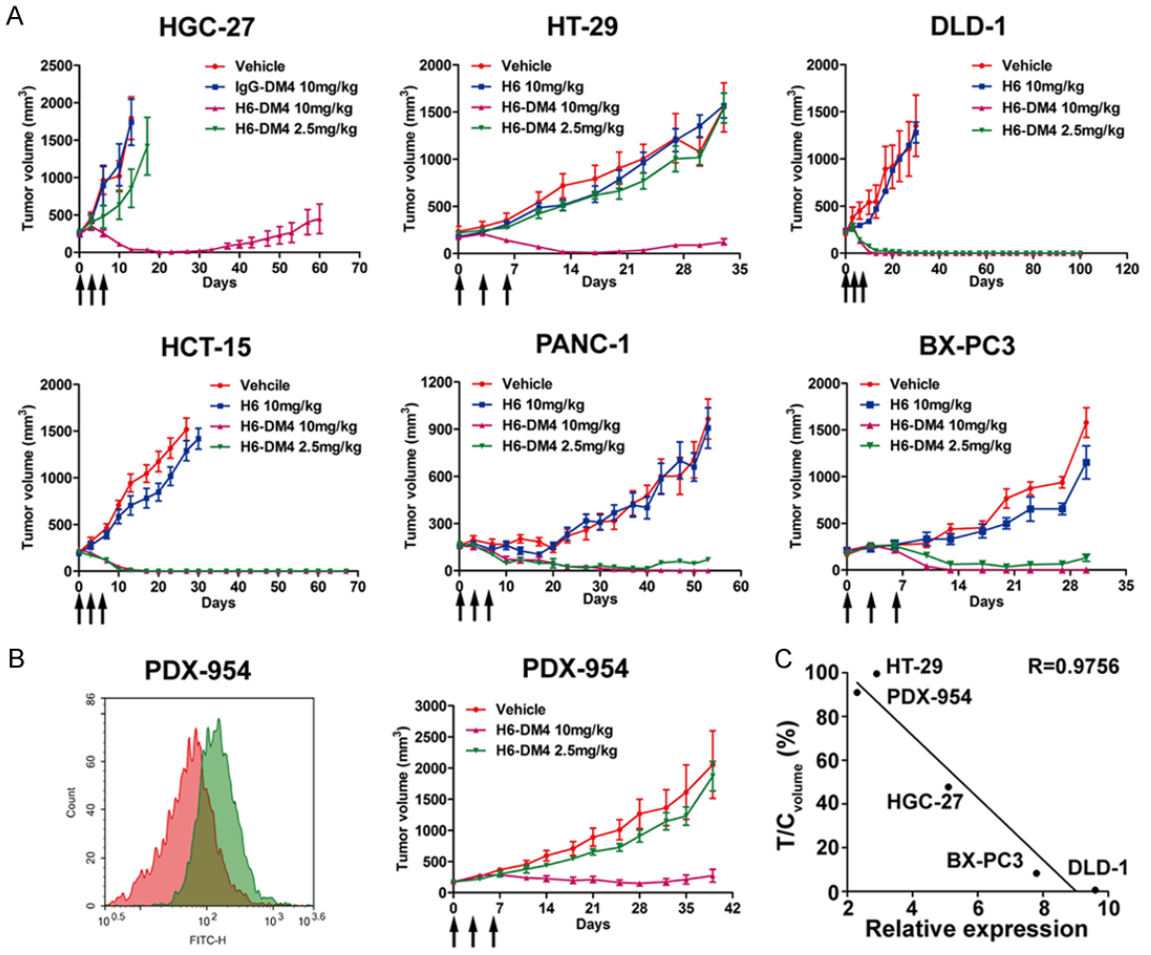

Figure 5. Antitumor efficacy of H6-DM4 in established subcutaneous xenografts. A. Dosed once as indicated (black arrow) with H6-DM4 (10 mg/kg or 2.5 mg/kg), vehicle (PBS), IgG-DM4 (10 mg/kg) or H6 (10 mg/kg) on a Q3D × 3 regimen in HGC-27 gastric cancer; HT-29, DLD-1, and HCT-15 colorectal cancer; PANC-1 and BX-PC3 pancreatic cancers. B. 5T4 expression was confirmed in PDX-954 by FCM. Mice bearing PDX-954 tumor fragments were treated with H6-DM4 (2.5 mg/kg or 10 mg/kg), IgG-DM4 (10 mg/kg) or H6 (10 mg/kg), vehicle (PBS) on a Q3D × 3 regimen. C. *In vivo* efficacy correlated with 5T4 expression in GI cancer. *In vivo* efficacy of H6-DM4 (2.5 mg/kg, Q3D × 3), indicated as treatment to control ratio (T/C_{volume}) of tumor growth, plotted against 5T4 expression of five GI cancer xenograft models as determined by FCM.

immunotherapy such as ADC [12, 24, 27]. Here, we identified high expression of 5T4 in gastric carcinoma, colorectal cancer, and pancreatic cancer, which negatively correlated with overall survival of GI cancer patients, suggesting 5T4 might be closely related to tumor malignancy, thus patients with aggressive cancers might benefit from 5T4-targeting ADC. All of these prompted us to explore a 5T4-targeting ADC for gastrointestinal cancer. In consideration of the tough challenges for treatment of solid tumors, A novel anti-5T4 monoclonal antibody was generated and conjugated to the potent microtubule inhibitor DM4. We evaluated the therapeutic efficacy of the ADC on GI cancer by establishing multiple xenograft models. Considering the resistance and recurrence of GI cancer, we further challenged H6-DM4 with colorectal cancer-initiating cells and cancer cells resistant to chemotherapy. CICs and resistant cells were effectively eradicated by H6-DM4. Hence the ADC may have the potential for therapy of GI cancer.

ADC is composed of three parts: antibody, payload, and linker, which employed two advantages: high efficiency of chemical drugs and specificity of antibodies. Though four ADCs have been approved by FDA, no common rationales have arrived for designs of ADCs. In this study, we generated a novel anti-5T4 antibody with high affinity and rapid internalization

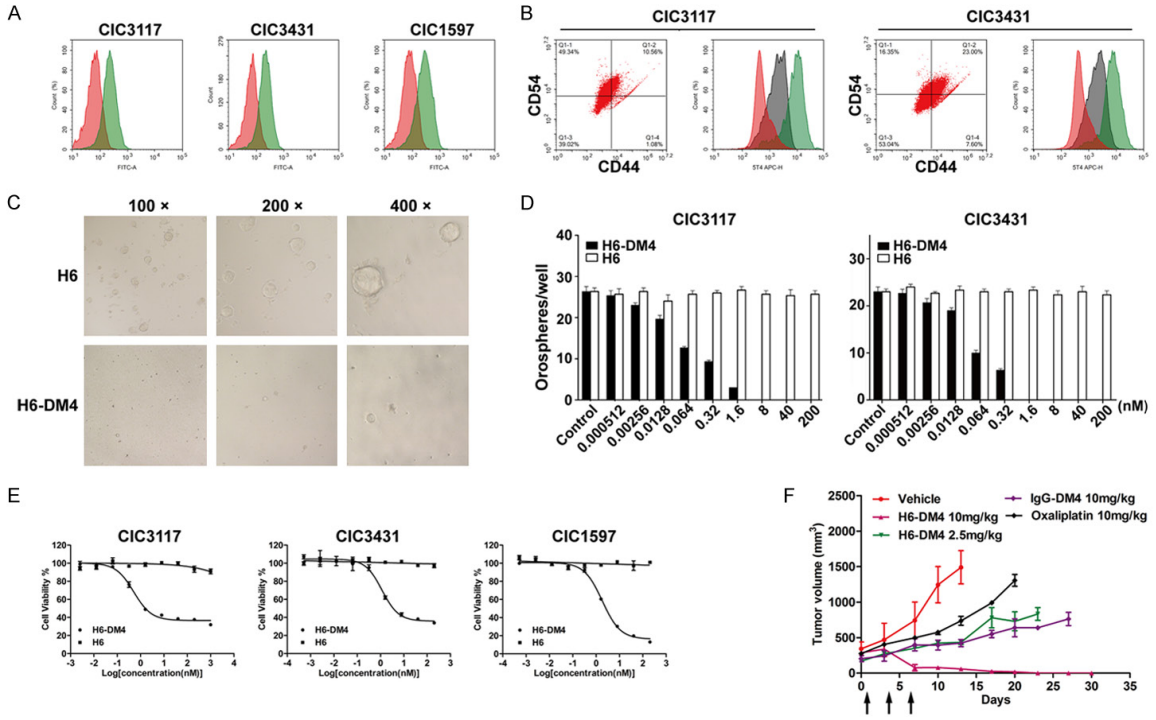

Figure 6. Antitumor activity of H6-DM4 in colorectal CICs *in vitro* and *in vivo*. A. FCM analysis with hIgG (red) or H6 (green), respectively in colorectal CIC3117, CIC3431, and CIC1597. B. FCM analysis of 5T4 expression in CIC (green) and in non-CIC fractions (grey) of colorectal CIC3117 or CIC3431 with H6 or control IgG (red). C. In vitro cytotoxicity of H6-DM4 (solid circle) and control antibody H6 (solid square) against CIC3117, CIC3431, and CIC1597 colorectal CIC lines. Error bars represent SD of the mean. D. The number of CIC3117 or CIC3431 orospheres per well over 7 days after treatment with a 5-fold concentration gradient of H6-DM4 or H6 at 0.000512 nM, 0.00256 nM, 0.0128 nM, 0.064 nM, 0.32 nM, 1.6 nM, 8 nM, 40 nM and 200 nM. Error bars represent SD of the mean. E. H6-DM4 but not H6 induced a strong cytotoxicity in CIC3117 or CIC3431 *in vitro*. F. Tumor growth curves for CIC3431. Animals were dosed once as indicated (arrow) by intravenous injection (Q3D × 3) with H6-DM4 (2.5 mg/kg or 10 mg/kg), IgG-DM4 (10 mg/kg), standard-of-care chemotherapy oxaliplatin (10 mg/kg) or vehicle (PBS).

and then constructed a novel ADC, H6-DM4 that displayed a potent antitumor activity *in vitro* and in subcutaneous xenograft models. Administration of high doses of the naked anti-5T4 antibody or the control IgG-DM4 showed little impact on tumor growth, implying that H6-DM4 efficacy was mediated by targeted delivery of the payload to 5T4-positive tumor cells. But slight inhibition was observed in individual tumor xenografts treated with IgG-DM4 or H6 antibody, which could be owing to the enhanced permeability and retention (EPR) effect or immune response such as complement-dependent cytotoxicity (CDC) [28, 29].

In general, tumor cells with higher expression of 5T4 were more reactive to H6-DM4 *in vivo*. Weak efficacy in HT-29, HGC-27 and PDX-954 compared to that in DLD-1, HCT-15, PANC-1 and BX-PC3 models supported that 5T4 expression could act as a predictive marker for patient selection. Direct linear correlation between 5T4 expression level and efficacy was observed *in vivo* but not *in vitro* (**Table 1**; **Figure 5C**). Some tumor cells such as PANC-1 and HCT-15, though with higher expression of 5T4, did not get excellent results treated with H6-DM4 *in vitro*, possibly because these cells had relatively slower internalization rate: 26% and 23%, respectively (Supplementary Figure 7). However, durable tumor regressions were observed in the two xenograft models. That the efficacy of PANC-1 and HCT-15 was not consistent *in vitro* and *in* vivo may be due to the discrepant kinetics of drug exposure under different conditions [30]. In addition, H6-DM4 displayed more pronounced antitumor activity for DLD-1 both *in vitro* and in xenograft models, which may own to high expression of 5T4 and excellent internalization ability of H6 in DLD-1 cell (**Figures 2** and **3E**; **Table 1**).

Cancer stem cells (also called cancer-initiating cells) are implicated in tumor initiation, maintenance, and recurrence, leading to the

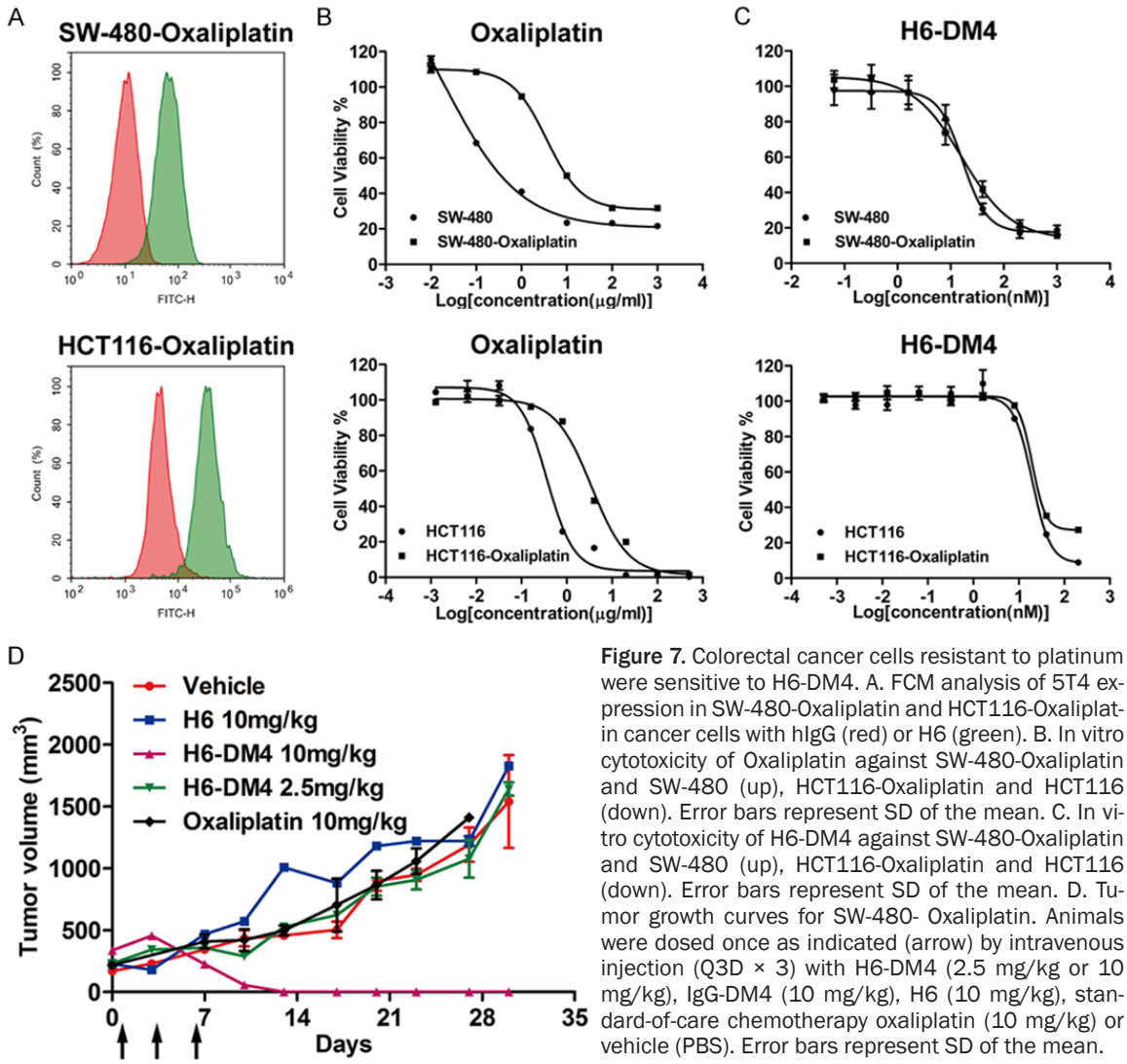

Figure 7. Colorectal cancer cells resistant to platinum were sensitive to H6-DM4. A. FCM analysis of 5T4 expression in SW-480-Oxaliplatin and HCT116-Oxaliplatin cancer cells with hIgG (red) or H6 (green). B. In vitro cytotoxicity of Oxaliplatin against SW-480-Oxaliplatin and SW-480 (up), HCT116-Oxaliplatin and HCT116 (down). Error bars represent SD of the mean. C. In vitro cytotoxicity of H6-DM4 against SW-480-Oxaliplatin and SW-480 (up), HCT116-Oxaliplatin and HCT116 (down). Error bars represent SD of the mean. D. Tumor growth curves for SW-480- Oxaliplatin. Animals were dosed once as indicated (arrow) by intravenous injection (Q3D × 3) with H6-DM4 (2.5 mg/kg or 10 mg/kg), IgG-DM4 (10 mg/kg), H6 (10 mg/kg), standard-of-care chemotherapy oxaliplatin (10 mg/kg) or vehicle (PBS). Error bars represent SD of the mean.

poor effect of standard chemotherapies and tumor recurrence [31]. 5T4 was reported as a potential marker of CSCs in NSCLC squamous cell carcinoma [15]. 5T4-targeting ADC MEDI0641 could effectively kill cancer stem cells and non-cancer stem cells, resulting in regression of tumors such as breast cancer, head and neck squamous cell carcinoma, etc [12, 27]. In this study, we demonstrated that 5T4 expression was higher in CICs than that in non-CICs in colorectal cancer, which could be a new marker for colorectal CICs. H6-DM4 functioned to eliminate CICs induced tumor xenograft, suggesting that our ADC may prevent the recurrence caused by residual CICs.

Resistance to chemotherapeutic agents is the leading cause of recurrence in GI cancer [32, 33]. One of the mechanisms of resistance is an increased cellular efflux, such as P-glycoprotein (P-gp) and multidrug resistance-associated protein 2 [34, 35]. Here, that tumor cells were resistant to oxaliplatin but sensitive to H6-DM4 was probably because the payload constantly accumulated in the cells through antibody-mediated internalization. Additionally, it was reported that microtubule inhibitor with higher binding affinity might be an effective strategy to overcome drug resistance [36]. Thus, DM4, as a powerful microtubule inhibitor, was utilized to conjugate to an efficiently internalized antibody to counteract treatment resistance.

The design of ADC is much more complicated than a simple linkage of a mAb to a payload. The considerations include target characteri-

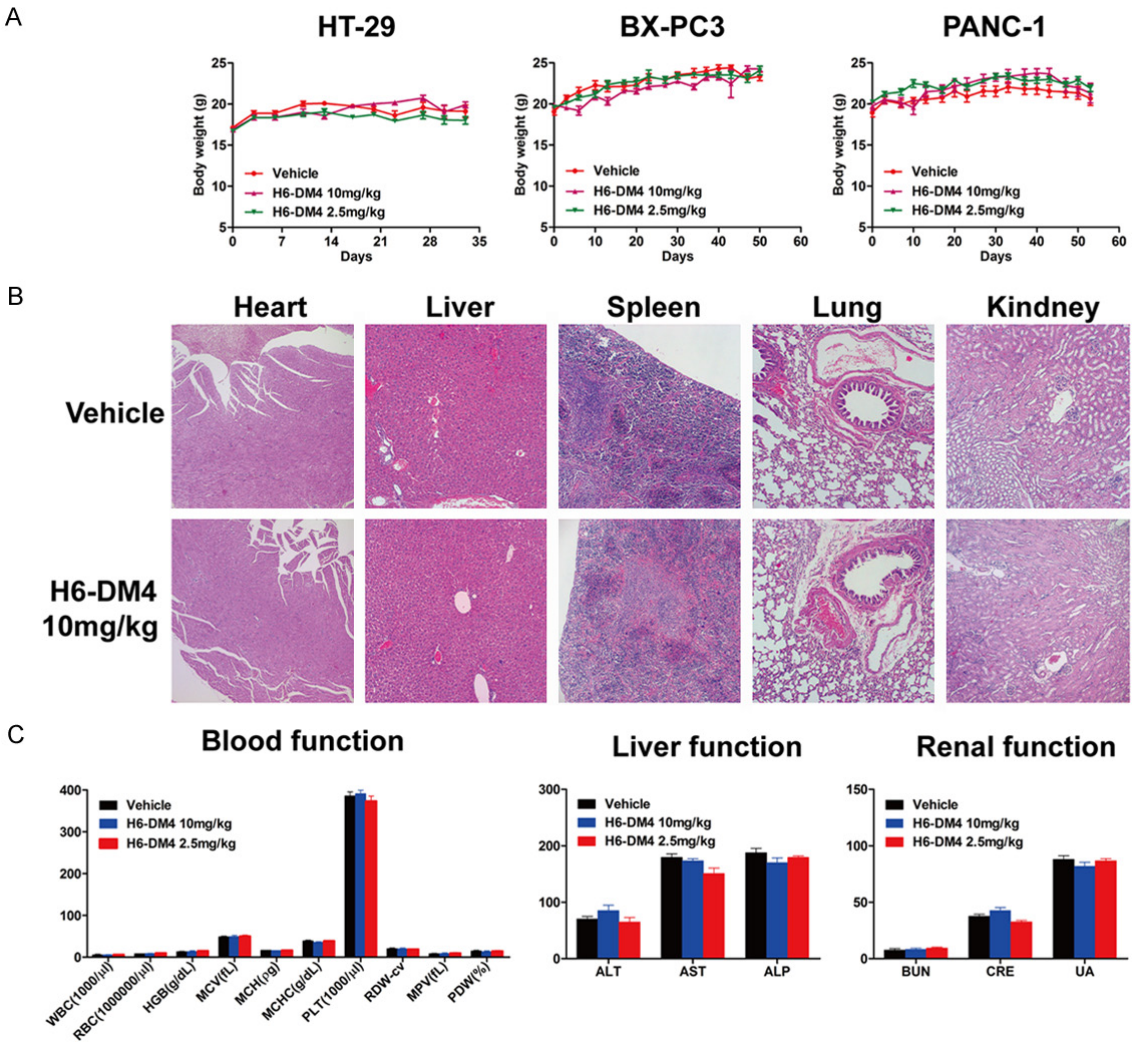

Figure 8. Preliminary safety evaluation of H6-DM4. A. Graphs showed mean mouse weight over time in HT-29, BX-PC3, and PANC-1 models after treatment with H6-DM4 (2.5 mg/kg, 10 mg/kg) and vehicle (PBS). Error bars represent SD of the mean. B. H&E images of vital organ of mice at 3 days after treatment with either 10 mg/kg H6-DM4 or vehicle (PBS). Magnification: × 100. C. The graph depicted blood function, liver function, and renal function 3 days after 2.5 mg/kg H6-DM4, 10 mg/kg H6-DM4 or vehicle injection. Error bars represent SD of the mean.

zation, antibody properties, payload, and linker. All three components of an ADC need to be optimized to achieve the best combination. In this study, we developed a novel anti-5T4 antibody H6 with higher affinity and fast internalization and made a new combination of antibody and payload. Of note, the resulting ADC was capable of selectively killing 5T4-positive cancer-initiating cells and drug-resistant cells *in vitro* and *in vivo*. In addition, it was able to induce a bystander effect on neighboring 5T4-negative tumor cells through a lipophilic payload S-methyl-DM4 [37, 38], which might explain the durable therapeutic efficacy of H6-DM4, even if a heterogeneous expression of 5T4 was observed in some GI cancer tissues (Supplementary Figure 8). Collectively, our studies demonstrate that H6-DM4 may be an effective ADC for the treatment of GI cancer.

Acknowledgements

This work is supported by National Major Scientific and Technological Special Project [grant number 2007ZX09302-010-005-003] and National Natural Science Foundation of China [grant numbers 81372822, 81501368 and 81672722]. The authors gratefully acknowledge Prof. Xianming Mo for providing colorectal CICs. The authors thank Prof. Feng Bi for providing SW-480-Oxaliplatin and HCT116-Oxaliplatin cell lines; Fan Yang (Jinkai biotechnol-

ogy company) for the mass spectrometric analysis; Min Wu for improving this manuscript; Hao Chen, Qiang Chen, and Dan Su for their help in the experiments and data analysis. Finally, the authors acknowledge technical expertise of Yingbin Zhao for IHC.

The study with tumor samples obtained from mice was approved by Institutional Animal Care and Treatment Committee of Sichuan University, China.

Disclosure of conflict of interest

None.

Abbreviations

GI, Gastrointestinal; ADC, Antibody-Drug Conjugate; CICs, Cancer-Initiating Cells; CSCs, Cancer Stem Cells; IHC, Immunohistochemistry; PDX, Patient-Derived Xenograft; FCM, Flow Cytometry; CHO, Chinese Hamster Ovary; DM4, N2'-deacetyl-N2'-(4-mer-capto-4-methyl-1-oxopentyl)-maytansine; DARs, Drug-Antibody Ratios; STR, Short Tandem Repeat; CDC, Complement-Dependent Cytotoxicity; EPR, Enhanced Permeability and Retention; MFI, Mean Fluorescence Intensity; ECD, Extracellular Domain.

Address correspondence to: Jinliang Yang, State Key Laboratory of Biotherapy and Cancer Center/ Collaborative Innovation Center for Biotherapy, West China Hospital, Sichuan University, 3-17 People Road, Chengdu 610041, China. Tel: + 86 28 855-02796; Fax: +86 28 85502796; E-mail: jlyang01@163.com

References

[1] Van Cutsem E, Sagaert X, Topal B, Haustermans K, Prenen H. Gastric cancer. Lancet 2016; 388: 2654-2664.
[2] Rahman R, Asombang AW, Ibdah JA. Characteristics of gastric cancer in Asia. World J Gastroenterol 2014; 20: 4483-90.
[3] Kraus S, Nabiochtchikov I, Shapira S, Arber N. Recent advances in personalized colorectal cancer research. Cancer Lett 2014; 347: 15-21.
[4] Fakih MG. Metastatic colorectal cancer: current state and future directions. J Clin Oncol 2015; 33: 1809-24.
[5] Ansari D, Gustafsson A, Andersson R. Update on the management of pancreatic cancer: surgery is not enough. World J Gastroenterol 2015; 21: 3157-65.
[6] Kamisawa T, Wood LD, Itoi T, Takaori K. Pancreatic cancer. Lancet 2016; 388: 73-85.
[7] Shefet-Carasso L, Benhar I. Antibody-targeted drugs and drug resistance--challenges and solutions. Drug Resist Updat 2015; 18: 36-46.
[8] Thomas A, Teicher BA, Hassan R. Antibody-drug conjugates for cancer therapy. Lancet Oncol 2016; 17: e254-e262.
[9] Griffiths RW, Gilham DE, Dangoor A, Ramani V, Clarke NW, Stern PL, Hawkins RE. Expression of the 5T4 oncofoetal antigen in renal cell carcinoma: a potential target for T-cell-based immunotherapy. Br J Cancer 2005; 93: 670-7.
[10] Stern PL, Harrop R. 5T4 oncofoetal antigen: an attractive target for immune intervention in cancer. Cancer Immunol Immunother 2017; 66: 415-426.
[11] Southall PJ, Boxer GM, Bagshawe KD, Hole N, Bromley M, Stern PL. Immunohistological distribution of 5T4 antigen in normal and malignant tissues. Br J Cancer 1990; 61: 89-95.
[12] Kerk SA, Finkel KA, Pearson AT, Warner KA, Zhang Z, Nör F, Wagner VP, Vargas PA, Wicha MS, Hurt EM. 5T4-targeted therapy ablates cancer stem cells and prevents recurrence of head and neck squamous cell carcinoma. Clin Cancer Res 2017; 23: 2516-2527.
[13] Starzynska T, Marsh P, Schofield PF, Roberts SA, Myers KA, Stern PL. Prognostic significance of 5T4 oncofetal antigen expression in colorectal carcinoma. Br J Cancer 1994; 69: 899-902.
[14] Castro FV, McGinn OJ, Krishnan S, Marinov G, Li J, Rutkowski AJ, Elkord E, Burt DJ, Holland M, Vaghjiani R. 5T4 oncofetal antigen is expressed in high risk of relapse childhood pre-B acute lymphoblastic leukemia and is associated with a more invasive and chemotactic phenotype. Leukemia 2012; 26: 1487-1498.
[15] Damelin M, Geles KG, Follettie MT, Yuan P, Baxter M, Golas J, DiJoseph JF, Karnoub M, Huang S, Diesl V, Behrens C, Choe SE, Rios C, Gruzas J, Sridharan L, Dougher M, Kunz A, Hamann PR, Evans D, Armellino D, Khandke K, Marquette K, Tchistiakova L, Boghaert ER, Abraham RT, Wistuba, II, Zhou BB. Delineation of a cellular hierarchy in lung cancer reveals an oncofetal antigen expressed on tumor-initiating cells. Cancer Res 2011; 71: 4236-46.
[16] Kozovska Z, Gabrisova V, Kucerova L. Colon cancer: cancer stem cells markers, drug resistance and treatment. Biomed Pharmacother 2014; 68: 911-916.
[17] Vidal SJ, Rodriguez-Bravo V, Galsky M, Cordon-Cardo C, Domingo-Domenech J. Targeting cancer stem cells to suppress acquired chemotherapy resistance. Oncogene 2014; 33: 4451-63.
[18] Ward CM, Eastham AM, Stern PL. Cell surface 5T4 antigen is transiently upregulated during early human embryonic stem cell differentia-

tion: effect of 5T4 phenotype on neural lineage formation. Exp Cell Res 2006; 312: 1713-26.
[19] Barrow KM, Ward CM, Rutter J, Ali S, Stern PL. Embryonic expression of murine 5T4 oncofoetal antigen is associated with morphogenetic events at implantation and in developing epithelia. Dev Dyn 2005; 233: 1535-45.
[20] Nieto MA, Cano A. The epithelial-mesenchymal transition under control: global programs to regulate epithelial plasticity. Semin Cancer Biol 2012; 22: 361-8.
[21] Kagermeier-Schenk B, Wehner D, Ozhan-Kizil G, Yamamoto H, Li J, Kirchner K, Hoffmann C, Stern P, Kikuchi A, Schambony A, Weidinger G. Waif1/5T4 inhibits Wnt/beta-catenin signaling and activates noncanonical Wnt pathways by modifying LRP6 subcellular localization. Dev Cell 2011; 21: 1129-43.
[22] Southgate TD, McGinn OJ, Castro FV, Rutkowski AJ, Al-Muftah M, Marinov G, Smethurst GJ, Shaw D, Ward CM, Miller CJ, Stern PL. CXCR4 mediated chemotaxis is regulated by 5T4 oncofetal glycoprotein in mouse embryonic cells. PLoS One 2010; 5: e9982.
[23] McGinn OJ, Marinov G, Sawan S, Stern PL. CXCL12 receptor preference, signal transduction, biological response and the expression of 5T4 oncofoetal glycoprotein. J Cell Sci 2012; 125: 5467-5478.
[24] Sapra P, Damelin M, Dijoseph J, Marquette K, Geles KG, Golas J, Dougher M, Narayanan B, Giannakou A, Khandke K, Dushin R, Ernstoff E, Lucas J, Leal M, Hu G, O'Donnell CJ, Tchistiakova L, Abraham RT, Gerber HP. Long-term tumor regression induced by an antibody-drug conjugate that targets 5T4, an oncofetal antigen expressed on tumor-initiating cells. Mol Cancer Ther 2013; 12: 38-47.
[25] Fan CW, Chen T, Shang YN, Gu YZ, Zhang SL, Lu R, OuYang SR, Zhou X, Li Y, Meng WT, Hu JK, Lu Y, Sun XF, Bu H, Zhou ZG, Mo XM. Cancer-initiating cells derived from human rectal adenocarcinoma tissues carry mesenchymal phenotypes and resist drug therapies. Cell Death Dis 2013; 4: e828.
[26] Zhang H, Wang Y, Wu Y, Jiang X, Tao Y, Yao Y, Peng Y, Chen X, Fu Y, Yu L. Therapeutic potential of an anti-HER2 single chain antibody-DM1 conjugates for the treatment of HER2-positive cancer. Signal Transduct Target Ther 2017; 2: 17015.
[27] Harper J, Lloyd C, Dimasi N, Toader D, Marwood R, Lewis L, Bannister D, Jovanovic J, Fleming R, D'Hooge F, Mao S, Marrero AM, Korade M 3rd, Strout P, Xu L, Chen C, Wetzel L, Breen S, van Vlerken-Ysla L, Jalla S, Rebelatto M, Zhong H, Hurt EM, Hinrichs MJ, Huang K, Howard PW, Tice DA, Hollingsworth RE, Herbst R, Kamal A. Preclinical evaluation of MEDI0641, a pyrrolobenzodiazepine-conjugated antibody-drug conjugate targeting 5T4. Mol Cancer Ther 2017; 16: 1576-1587.
[28] Fan L, Campagnoli S, Wu H, Grandi A, Parri M, De Camilli E, Grandi G, Viale G, Pileri P, Grifantini R, Song C, Jin B. Negatively charged AuNP modified with monoclonal antibody against novel tumor antigen FAT1 for tumor targeting. J Exp Clin Cancer Res 2015; 34: 103.
[29] Gong X, Azhdarinia A, Ghosh SC, Xiong W, An Z, Liu Q, Carmon KS. LGR5-targeted antibody-drug conjugate eradicates gastrointestinal tumors and prevents recurrence. Mol Cancer Ther 2016; 15: 1580-90.
[30] Mao W, Luis E, Ross S, Silva J, Tan C, Crowley C, Chui C, Franz G, Senter P, Koeppen H. EphB2 as a therapeutic antibody drug target for the treatment of colorectal cancer. Cancer Res 2004; 64: 781-788.
[31] Hu YP, Fu LW. Targeting cancer stem cells: a new therapy to cure cancer patients. Am J Cancer Res 2012; 2: 340-356.
[32] Matuszcak C, Haier J, Hummel R, Lindner K. MicroRNAs: promising chemoresistance biomarkers in gastric cancer with diagnostic and therapeutic potential. World J Gastroenterol 2014; 20: 13658-66.
[33] Shang Y, Zhang Z, Liu Z, Feng B, Ren G, Li K, Zhou L, Sun Y, Li M, Zhou J, An Y, Wu K, Nie Y, Fan D. miR-508-5p regulates multidrug resistance of gastric cancer by targeting ABCB1 and ZNRD1. Oncogene 2014; 33: 3267-76.
[34] Hu T, Li Z, Gao CY, Cho CH. Mechanisms of drug resistance in colon cancer and its therapeutic strategies. World J Gastroenterol 2016; 22: 6876-89.
[35] Shi WJ, Gao JB. Molecular mechanisms of chemoresistance in gastric cancer. World J Gastrointest Oncol 2016; 8: 673-81.
[36] Yang CG, Barasoain I, Li X, Matesanz R, Liu R, Sharom FJ, Yin DL, Díaz JF, Fang WS. Overcoming tumor drug resistance with high-affinity taxanes: a SAR Study of C2-modified 7-Acyl-10-deacetyl cephalomannines. Chem Med Chem 2007; 2: 691-701.
[37] Golfier S, Kopitz C, Kahnert A, Heisler I, Schatz CA, Stelte-Ludwig B, Mayer-Bartschmid A, Unterschemmann K, Bruder S, Linden L, Harrenga A, Hauff P, Scholle FD, Muller-Tiemann B, Kreft B, Ziegelbauer K. Anetumab ravtansine: a novel mesothelin-targeting antibody-drug conjugate cures tumors with heterogeneous target expression favored by bystander effect. Mol Cancer Ther 2014; 13: 1537-48.
[38] Nguyen M, Miyakawa S, Kato J, Mori T, Arai T, Armanini M, Gelmon K, Yerushalmi R, Leung S, Gao D, Landes G, Haak-Frendscho M, Elias K, Simmons AD. Preclinical efficacy and safety assessment of an antibody-drug conjugate targeting the c-RET Proto-Oncogene for breast carcinoma. Clin Cancer Res 2015; 21: 5552-62.

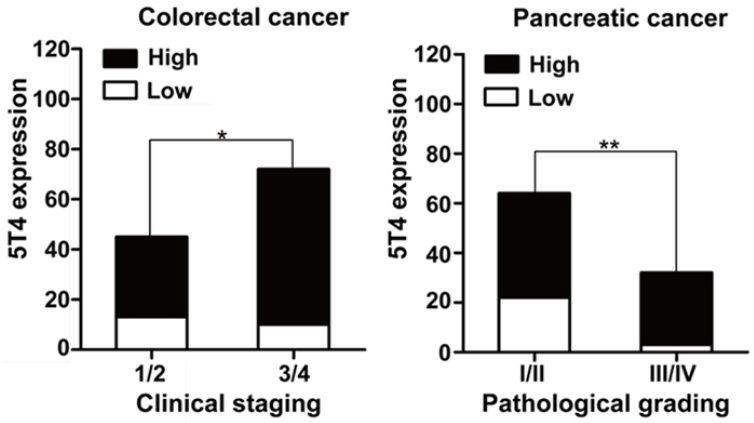

Supplementary Figure 1. The 5T4 expression levels correlated with pathological grading and clinical staging respectively in GI cancer. Chi-squared test represent 5T4 expression levels correlated with clinical staging (left, $P < 0.05$) in colorectal cancer and pathological grading (right, $P < 0.01$) in pancreatic cancer respectively. The white represents a low expression of 5T4, and the black represents a high expression of 5T4. $*P < 0.05$. $**P < 0.01$. $***P < 0.001$.

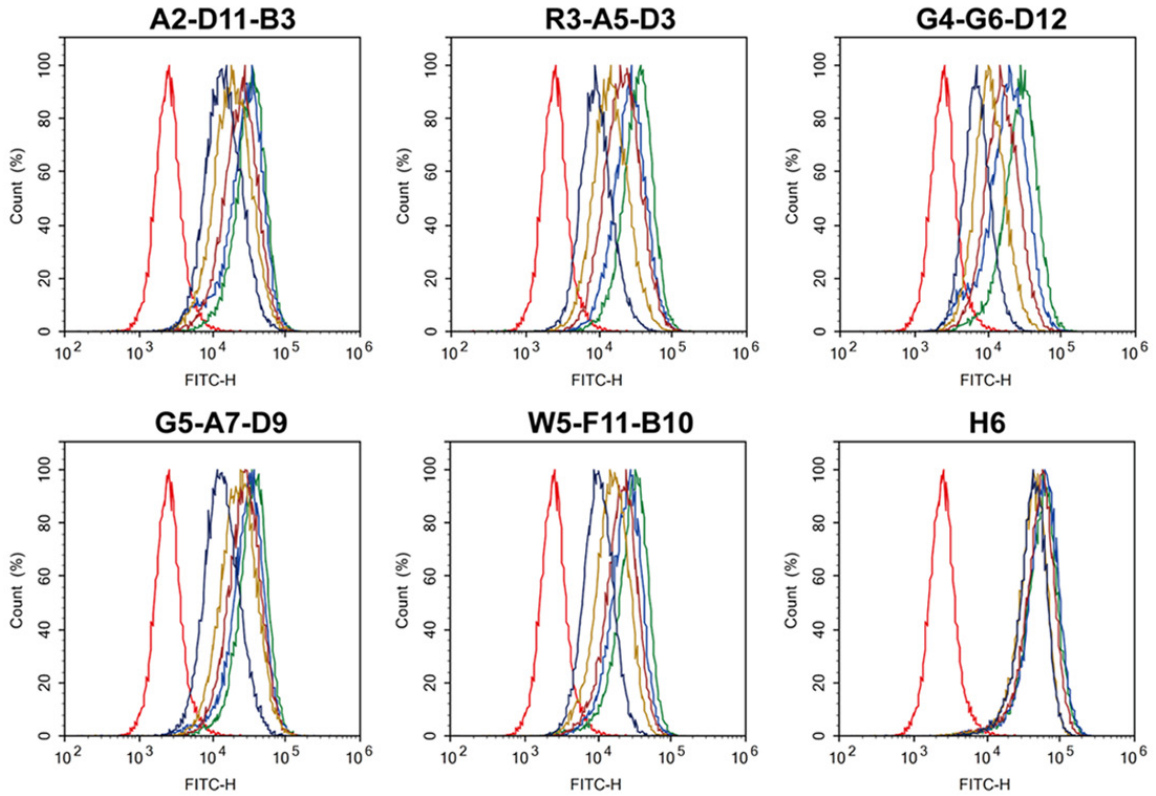

Supplementary Figure 2. Binding of some candidate antibodies to the cell surface of CHO-5T4$^+$ cells. FCM analysis of CHO-5T4$^+$ cells with control IgG (the far left) or each candidate antibody with different concentrations (32 μg/ml, 16 μg/ml, 8 μg/ml, 4 μg/ml, and 2 μg/ml, respectively). Names of antibodies are as follows: A2-D11-B3, R3-A5-D3, G4-G6-D12, G5-A7-D9, W5-F11-B10, and H6. The corresponding mean fluorescence intensity values are displayed in Supplementary Table 1.

Supplementary Table 1. Mean fluorescence intensity values of some candidate antibodies with different concentrations bond to CHO-5T4^{+} cells

Sample	Mean fluorescence intensity with different concentrations				
	32 μg/ml	16 μg/ml	8 μg/ml	4 μg/ml	2 μg/ml
A2-D11-B3	37,488	32,195	28,189	22,733	17,180
R3-A5-D3	38,268	30,544	25,200	17,499	10,944
G4-G6-D12	32,267	22,296	18,418	12,548	8,201
G5-A7-D9	40,079	34,459	31,710	27,193	16,277
W5-F11-B10	33,406	27,716	23,834	18,153	11,700
H6	65,816	64,089	58,481	46,612	46,830
Mouse control			2,855		

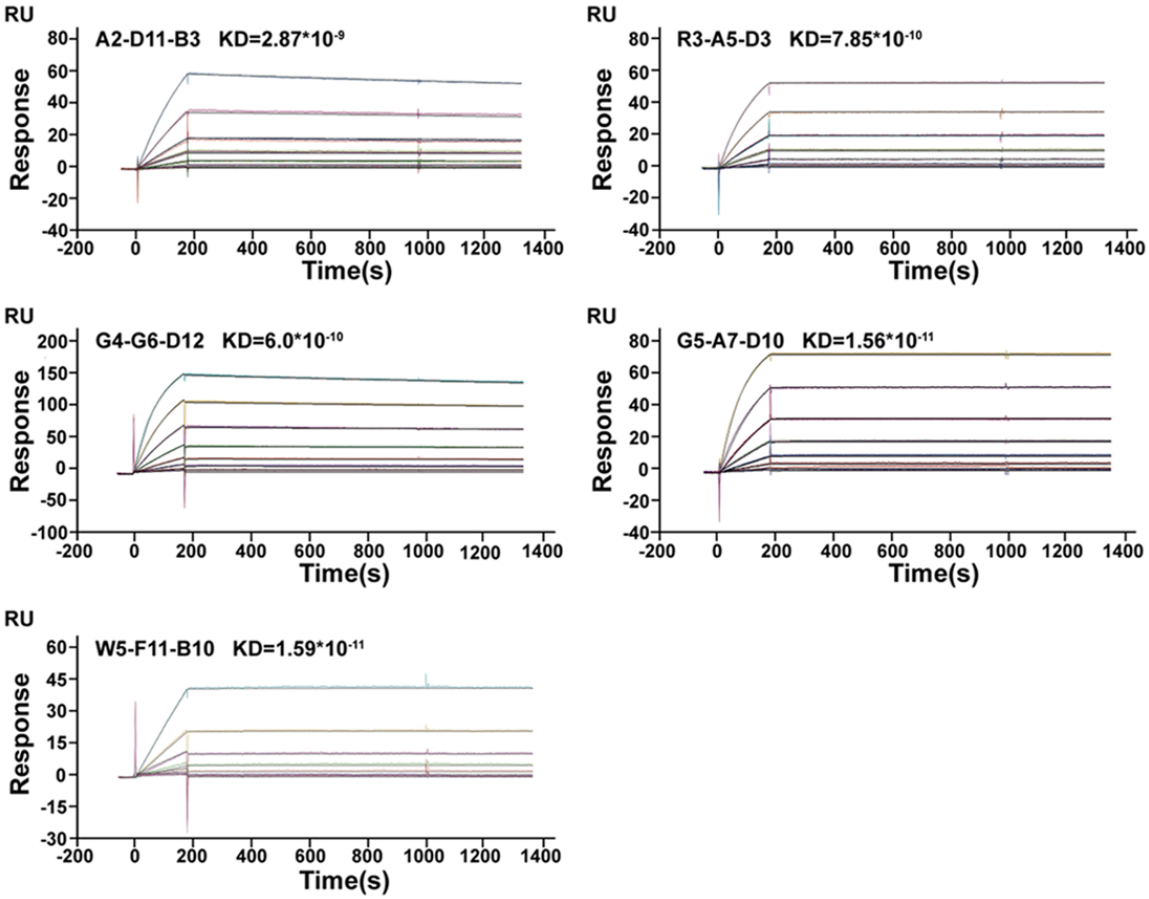

Supplementary Figure 3. Affinity analysis of some candidate antibodies by SPR. Names of antibodies are as follows: A2-D11-B3, R3-A5-D3, G4-G6-D12, G5-A7-D9, and W5-F11-B10. Each antibody was assayed at different concentrations (0.25 nM, 0.5 nM, 1 nM, 2 nM, 4 nM, 8 nM, 16 nM, and 32 nM).

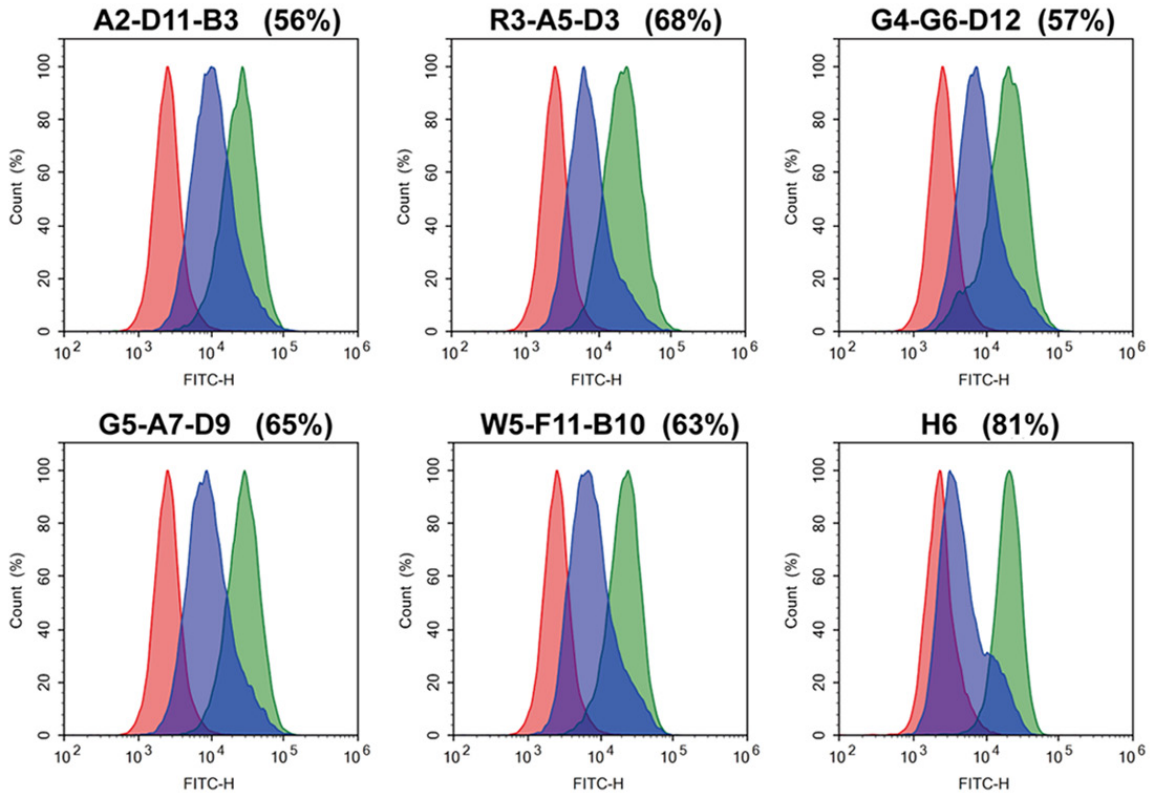

Supplementary Figure 4. Internalization rate of some candidate antibodies. Names of antibodies are as follows: A2-D11-B3, R3-A5-D3, G4-G6-D12, G5-A7-D9, W5-F11-B10, and H6. The red represents cells incubated with control IgG; the green with each antibody remained on ice; the blue with the corresponding antibody shifted to 37 °C for 4 h.

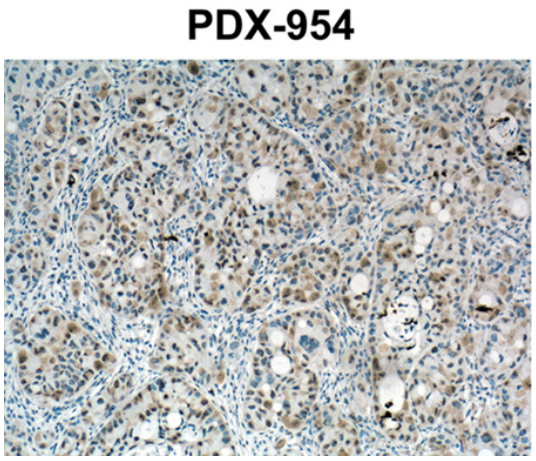

Supplementary Figure 5. 5T4 expression of PDX-954 by IHC. 5T4 expression was confirmed in PDX-954 by IHC. Magnification: × 100.

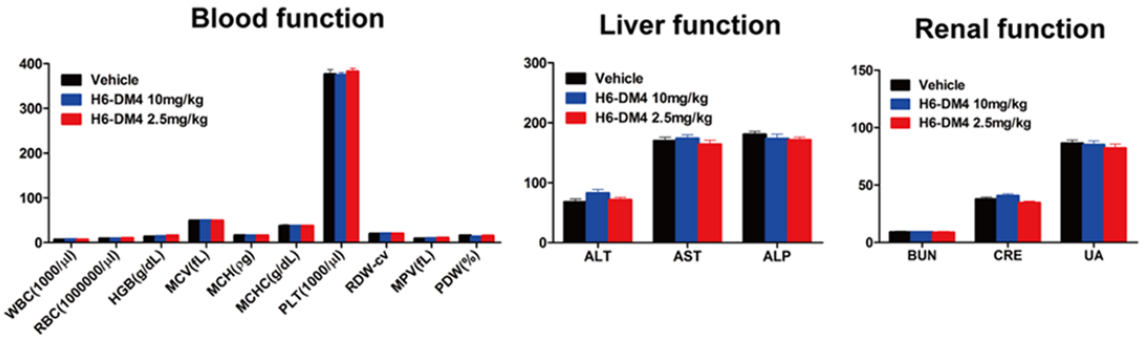

Supplementary Figure 6. Preliminary safety evaluation of H6-DM4 on day 29. The graph depicted blood function, liver function, and renal function 29 days after treatment with 2.5 mg/kg H6-DM4, 10 mg/kg H6-DM4, and vehicle (Q3D × 3). Error bars represent SD of the mean.

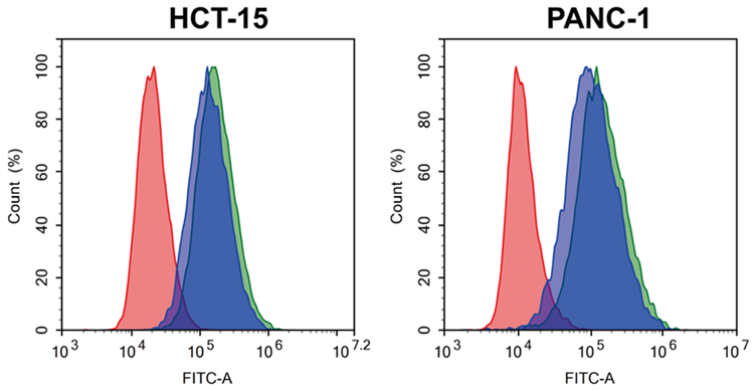

Supplementary Figure 7. Four-hour internalization rate of HCT-15 and PANC-1 cells. Flow cytometry-based *in vitro* internalization assay was used to determine the relatively low internalization rate of H6 in HCT-15 and PANC-1 cells (23% and 26%, respectively). The red represents cells incubated with isotype IgG; the green with H6 remained on ice; the blue with H6 shifted to 37 °C for 4 hours.

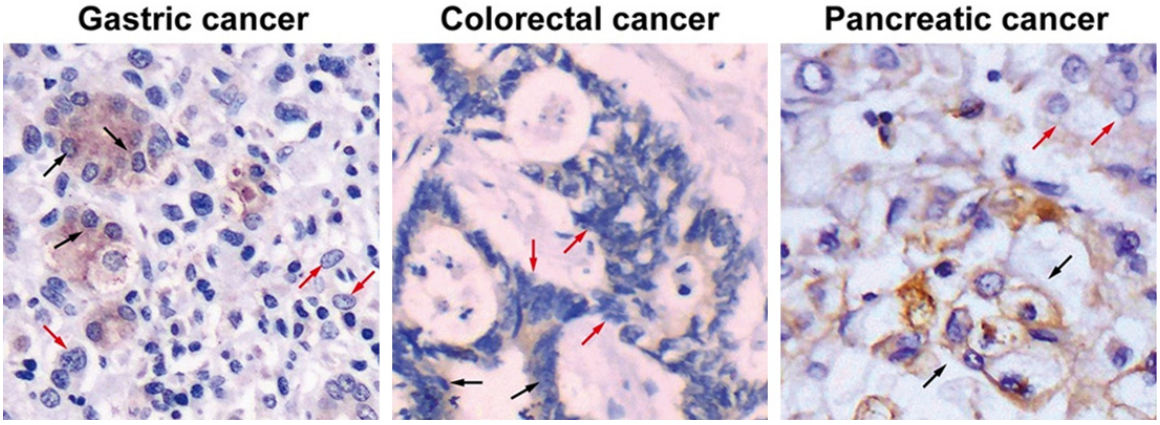

Supplementary Figure 8. 5T4 protein heterogeneity in GI cancer. The IHC results represent intra-tumor 5T4 heterogeneity in some gastric tumors (left), colorectal tumors (center) and pancreatic tumors (right). The black arrow represents tumor cells that are brown stained, and the red arrow represents tumor cells that are not brown stained. Magnification: × 400.